International Journal of Scientific Research Updates

Journal homepage: https://orionjournals.com/ijsru/

ISSN: 2783-0160 (Online)

(Research Article)

Biosynthesis of silver nanoparticles using *Cissus aralioides* Methanol leaf extract and antimicrobial application

Innocent Chukwujekwu Onunkwo [1,*], Mary Olire Edema [2], Christiana E. Ogwuche [2] and Edith A. Enemose [1]

[1] *Department of Industrial Chemistry, Nigeria Maritime University, Okerenkoko, Delta State, Nigeria.*

[2] *Department of Chemistry, Federal University of Petroleum Resources, Effurun, Delta State, Nigeria.*

International Journal of Scientific Research Updates, 2026, 11(01), 020-033

Publication history: Received on 27 January 2026; revised on 06 March 2026; accepted on 06 March 2026

Article DOI: https://doi.org/10.53430/ijsru.2026.11.1.0013

Abstract

Materials manipulated to nanoscale have demonstrated to have improved properties, and functionality in several applications. In this study, *Cissus aralioides* leaf was extracted with methanol through Soxhlet extraction method. The extract was utilized in a biosynthetic process with silver nitrate, under regulated temperature and constant monitoring, to obtain the silver nanoparticles (AgNPs). The NPs was characterized using UV-visible spectrophotometer, FT-Infrared (FTIR) spectrometer, Powered X-ray Diffractometer (PXRD), Scanning Electron Microscope (SEM), Energy-Dispersive X-ray (EDX), and Transmission Electron Microscope (TEM). Then, the NPs' antimicrobial activity against *Escherichia coli*, *Staphylococus aureus*, *Candida albicans*, and *Aspergillus fumigatus*, was conducted using Agar-well diffusion method, at 100, 200, 300, and 400 mg/mL. The biosynthesized Ag nanoparticles showed a wavelength max of 375 nm with a calculated bandgap energy of 3.30 eV, suitable for nanoelectronic applications, and semiconductor fabrications. Numerous bands of functional groups, including O-H, C=O, C-H, and others, were visible in the FTIR spectrum. The NPs also displayed an uneven and rough surface for the SEM data, and the predominant element was silver (89.87 %), as shown by the EDX result. Its average crystalline size was 22.52 nm, with mean particle size calculated from TEM image at 3.20 nm. The AgNPs demonstrated strong effects against the microbes, with the highest activity against the *Candida albicans*. The highest sensitivity was at 22 mm, and the estimated minimum inhibitory concentration was 100–200 mg/mL. Amid other promising applications, the NPs has proven that it can be used to control pathogenic microbes.

Keywords: *Cissus aralioides*; Methanol extract; Silver; Nanoparticles; Microbes; Antimicrobial activity

1. Introduction

There has been increase in synthesis of nanoparticles and their applications in the recent years which is as a result of their small size (ranges from 1-100nm), increased surface area as well as reactivity [1–3]. Nanoparticles' synthesis can be chemical, biological or physical [4]. Nanomaterials can be successfully made from noble metals such as Cu, Ag, Gold, Titanium, etc. [5], and they various technological applications. The technology has the ability to transform biologically active chemicals that are labile, poorly soluble, and poorly absorbed into promising deliverables, nanoparticle technologies hold considerable promise [6]. Nanoparticles (NPs) find extensive use in the disciplines of biology, electronics, and optics. They have demonstrated their effectiveness in a variety of fields, including medicine, pharmacy, energy, tissue engineering, electronics, environment, biomolecules, protein diagnostics, cellular engineering, and more [7]. Biological synthesis of nanoparticles using medicinal plant materials is the most highly recommended, and it is gaining traction because it is an eco-friendly approach and also presents improved materials with several potential properties and applications.

* Corresponding author: Innocent Chukwujekwu Onunkwo

Cissus aralioides is a vine and medicinal plant that belongs to the family of *Vitaceae*. Every part of the plant is termed to possess health benefits. The plant has been used to provide remedies to health issues like pain, swelling, arthritis and rheumatism, and the solvent extracts of the stem have displayed activities against some pathogenic microorganisms [8–9]. The Nigeria's Igbo tribe calls the plant "Eriri Agwo" and the plant's leaf is used extensively by Nigerian Folklorists to treat swelling and microbial infection as well as wounds, and plant sap used as eye drops for eye diseases [10–11]. The plant's leaf is edible and non-toxic, and possesses a lot of phytochemicals [12]. The plant is commonly called "Kindamina" in Cameroon, and Cameroon herbalists also use the leaf and root of the plant to combat urogenital and gastrointestinal tracts infections [13]. The triturated leaves of the plant have also been used in Gabon to treat gonorrhea when mixed with sugarcane juice; and in Congo Brazzaville, it is employed in relieving cough, fever and treatment of some kidney problems [9]. The seed oil of the plant has a good saponification, acid, iodine, peroxide and free fatty acid values necessary for cosmetics and pharmaceutical application; in addition to low turbidity, good moisture content, relative density and refractive index values [14]. The seed oil of *Cissus aralioides* is yellowish liquid and it is classified as a non-drying oil (given its low iodine value); thus, can be employed in production of cosmetics products, and lubricants, due to its low content of unsaturated fatty acids [14]. The plant has also demonstrated to possess antioxidant [15–17], and anti-inflammatory properties [11, 18–21]. A constituent (Aralioidamide A) isolated from the plant's stem, has demonstrated antimicrobial activity [22].

A lot of medicinal plant extracts of *Aloe vera* [23], *Cinnamomum verum* [24], *Ananas comosus* [25], *Moringa oleifera* [26], *Lippia adoensis* [27], *Ipomoea carnea* Jacq [3], *Opuntia ficus indica* [28], have been utilized in the synthesis of nanoparticles and they have displayed interesting antimicrobial properties. According to reports, silver nanoparticles are not harmful to people, but they do prevent the growth of viruses, bacteria, and other eukaryotic microbes [29–30], thus capable of preserving materials they are incorporated from deterioration by pathogenic microorganisms. Silver nanoparticles are utilized in sunscreen lotions, textile industries, water treatment, antibacterial treatments, and more [31].

2. Materials and methods

2.1. Materials

The plant (*Cissus aralioides*) leaves were authenticated (and DELSU-0301, assigned) by a taxonomist from Delta State University's Herbarium Unit in Abraka, Delta State, Nigeria, before being utilized in the experiment. Perkin Elmer Lambda 40 UV-visible Spectrometer, Pelkin Elmer 3000 MX Fourier Transform Infra-red (FTIR) Spectrometer, Rigaku D/Max-lllC Powered X-ray diffractometer (pXRD - developed by Rigaku Int. Corp. Tokyo, Japan), JOEL JSM-7600F Scanning Electron Microscope (SEM), EDX-8100 Energy Dispersive X-ray (EDX) Spectrometer, and JEM-ARM200F-G-TEM Transmission Electron Microscope (TEM) were used for spectroscopic characterization purposes; Other reagents used were of analytical grades, in addition to Mueller–Hinton agar (MHA) base medium (purchased from Merck, Germany) and used for the antimicrobial screening. The microorganisms used are *Staphylococcus aureus*, *Escherichia coli*, *Candida albicans*, and *Aspergillus fumigatus* and they were obtained from Department of Microbiology, Delta State University, Abraka, Delta State. Gentamycin utilized as control medication was purchased from pharmacy store.

2.2. Methods

2.2.1 Extraction and Phytochemical Evaluation

A Soxhlet extraction procedure was performed on 200 g of fresh (paste form) leaf material with methanol (at 1:2 ratio) for 4 hours at 55°C. To obtain the crude extract, the extract mixture's solvent was evaporated (E3). To determine whether alkaloids, steroids, terpenoids, saponin, glycosides, anthraquinones, phenolic acids, carbohydrates, proteins, tannins, flavonoids, coumarins, and volatile oil were present, the extract was prepared using the phytochemical evaluation method outlined by Amina *et al*. [32], Jeenu *et al*. [33], and Onunkwo [34].

2.2.2 Preparation of the Ag Nanoparticles (AgNPs)

A mixture of 2000 mL of 10 mM $AgNO_3$ and 20 mL of a 10% (w/v) (100:1) methanolic extract of *Cissus aralioides* (E3) was continuously swirled on a magnetic stirrer for 10 minutes at 70 °C. The reduction mechanism was determined using the UV-Vis spectrometer, which monitored colour changes until the ideal reaction was reached. After that, in order to avoid autoxidation before purification, the AgNPs solution was moved to an amber-coloured bottle. The purified AgNPs was obtained by oven-drying the colloidal AgNPs solutions at 70 to 100 °C for two hours after centrifuging them at 4,000 rpm and continuously washing them with 10 mL of double-distilled water [3, 28].

2.2.3 Characterization of the Ag Nanoparticles (AgNPs)

Further preparations were performed before characterization of the NPs with Ultraviolet visible spectrophotometer, FTIR spectrometer, X-ray Diffraction, Scanning Electron Microscope, Energy Dispersive X-ray, and Transmission Electron Microscope (TEM) instruments [35].

UV–visible Spectrometric Analysis of the Ag Nanoparticles (AgNPs)

A Perkin Elmer Lambda 40 UV-visible spectrophotometer was used to analyze the biosynthesized AgNPs spectroscopically. The reduction of the $AgNO_3$ was also measured at intervals between 200 and 800 nm (using 1 mL of the suspension). Following purification, the sample (purified silver NPs) was diluted with deionized water (2 mL) and examined to obtain the spectrum with wavelength on the x-axis and absorbance on the y-axis [25, 28].

Fourier Transform Infrared (FTIR) Analysis of the Ag Nanoparticles

The dried and purified AgNPs was employed. For the FTIR examination of the dried AgNPs, potassium bromide (KBr) pellet (FTIR grade at a 1:100 ratio) was utilized. Using the Pelkin Elmer 3000 MX spectrometer, the spectrum was recorded. A 32 scans were performed at a resolution of 4 cm^{-1}. The 4500–300 cm^{-1} spectrum region was used to record the FT-IR spectrum of the silver NPs metal complex. The spectroscopic software Win-IR Pro Version 3.0 was used to analyze the IR spectrum with a peak sensitivity of 2 cm^{-1} in order to extract the functional group data [25, 28, 36].

Powered X-ray Diffraction (PXRD) Analysis of the Ag Nanoparticles

The biologically reduced AgNPs (further powdered, pelletized, and sieved to 0.074 mm) was subjected to X-ray diffraction studies to ascertain their crystallinity. The Rigaku D/Max-lllC powered X-ray diffractometer (pXRD, Tokyo, Japan) was used to measure the crystallinity of the NPs coated onto glass slides. It was set to 40 kV and 20 mA and operated at a scanning rate of 2 ^{o}/min in the 2 to 50^{o} range at room temperature. When the X-ray passes through the sample, it produces peaks that are distinctive of the type of diffraction along a set of planes. The peculiarities of the atom arrangement within the sample determine how the peaks are diffracted. A comparison was made between the diffraction data (d value and relative intensity) and the standard data. Afterwards, the Debye–Scherrer equation was employed to calculate the average particle size of the AgNPs [25, 35, 36, 37].

Scanning Electron Microscope (SEM) Analysis of the AgNPs

A focused electron beam is used by the scanning electron microscope (SEM) to scan a sample's surface and provide an image of the sample. To do SEM analysis, JOEL JSM-7600F was used. Following conditioning (a platinum coating), the pure AgNPs was placed inside the specimen chamber. To capture the shape and texture of NPs, the pellet was then placed on the specimen stub (semiconductor wafer), and the SEM device placed the specimen in a chamber with a relatively high pressure. The working distance is short, and the electron optical column is differentially pumped to maintain a sufficiently low vacuum at the electron gun [25, 37].

Energy Dispersive X-ray (EDX) Analysis of the AgNPs

The EDX-8100 instrument was used to perform the EDX analysis and determine the AgNPs' elemental composition. To ascertain the elemental compositions, a thin layer of Ag NPs (about 10 mg/mL) was produced on a copper grid coated with carbon and analyzed [25, 36].

Transmission Electron Microscope (TEM) Analysis of the AgNPs

The JEM-ARM200F-G-TEM Transmission Electron Microscope (TEM) was used to view the nanoparticles' morphology. With an ultra-high resolution of 0.2 nm and a magnification of 2,000,000 X, the instrument was run at an accelerating voltage of 200 kV. The AgNPs was placed on carbon-coated copper grid, allowed to dry under a mercury lamp, and then magnified to create a TEM grid with a 3 mm diameter. In order to ascertain the size of the silver nanoparticles and provide unambiguous morphological information, the image magnifying software was then used to examine the particle size [25, 35–36].

2.2.4 Antimicrobial Activity

The antibacterial activity of the produced AgNPs against pathogenic microorganisms (*Staphylococcus aureus*, *Escherichia coli*, *Candida albicans*, and *Aspergillus fumigatus*) was evaluated using the agar-well diffusion method at doses of 100, 200, 300, and 400 mg/mL. The study was then conducted using cleaned and dried Petri dishes. A range of discs dipped in the various concentrations of the samples were arrayed outward on their individual inoculated Mueller-Hinton's agar plates. Furthermore, the standard antibiotics (Gentamycin) discs were used to treat prepared *E. coli, S.*

aureus, C. albicans, and *Aspergillus sp.* microbes at concentrations of 50, 25, 12.5, and 6.25 mg/mL, while the discs of ketoconazole were used to treat *C. albicans* and *Aspergillus sp.* at 250, 125, 62.5, and 31.25 mg/mL. The discs were then incubated at 37°C. Incubation was done according to the kind of microorganism in the samples (for example, fungi were incubated for five days, whereas bacteria were incubated for 24 hours). Following incubation, the zone of inhibition (ZOI) was observed and noted using callipers. Duplicate analysis was performed to ensure the activity was reliable [25, 28, 38].

3. Results and Discussion

3.1. Phytochemical Result

Flavonoids, alkaloids, steroids, phenols, tannins, anthraquinones, terpenoids, glycosides, carbohydrates, proteins, and volatile oil are among the phytochemicals found in the methanol leaf extract of *Cissus aralioides*; coumarin was not present (Table 1).

Table 1 Phytochemicals of methanol leaf extract of *Cissus aralioides* (E3)

Phytochemicals	Methanol Extract
Alkaloids	+
Steroids	+
Terpenoids	+
Flavonoids	+
Saponin	+
Tannins	+
Glycosides	+
Anthraquinones	+
Phenolic acids	+
Coumarin	-
Proteins	+
Carbohydrates	+
Volatile oil	+

Key: + = Present; - = Absent

According to reports, the plant contains flavonoids, alkaloids, steroids, tannins, terpenes, saponins, and cardiac glycosides [11, 39]. The plant's close relative, *Cissus hastata* (Semperai), has also been shown to contain tannin, alkaloids, phenolic compounds, and steroids [40]. Alkaloids from plants effectively treat skin conditions such seborrheic dermatitis, eczema, and neurodermatitis. They have also shown antibacterial qualities [11, 14, 41]. Inhibiting mediators and pathways that cause inflammation and cancer, such as nitric oxide synthase, lipooxygenase, and cyclooxygenase [7, 11], is another way that flavonoids have demonstrated strong anti-inflammatory properties. Steroids have also been shown to have anti-inflammatory; and tannins have also shown antioxidant and anti-inflammatory properties.

3.2. Characteristics of the Ag Nanoparticles

The *Cissus aralioides* extract's phytochemicals encouraged the bioreduction of $AgNO_3$, which resulted in the formation of NPs. Figure 1 illustrates the synthesis (A), and mechanism (B) of the Ag nanoparticles from the extract. The distinctive results of the NPs' UV-visible, FTIR, SEM, XRD, EDX, and TEM are then presented.

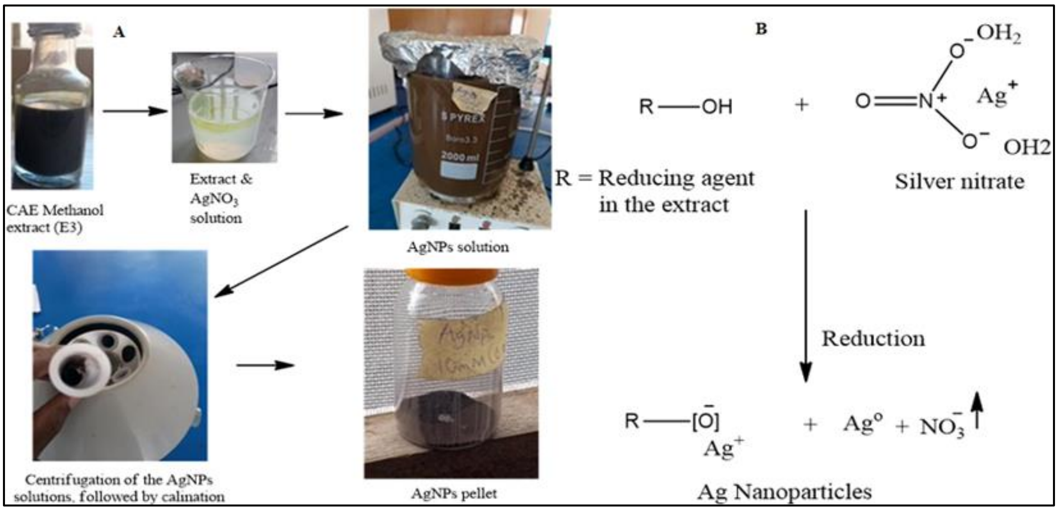

Figure 1 Synthesis (A), and mechanism (B) of the Ag Nanoparticles

3.2.1 UV–visible Spectrometric Results of the Ag Nanoparticles

UV-Vis spectrophotometer is a popular first instrumental method for monitoring the development of the nanoparticles. The reason for this is that it offers important details on how the NPs is formed. A UV-visible spectrometer (Perkin Elmer Lambda 40) was used to monitor the AgNPs' synthesis; the spectrum is displayed in Figure 2.

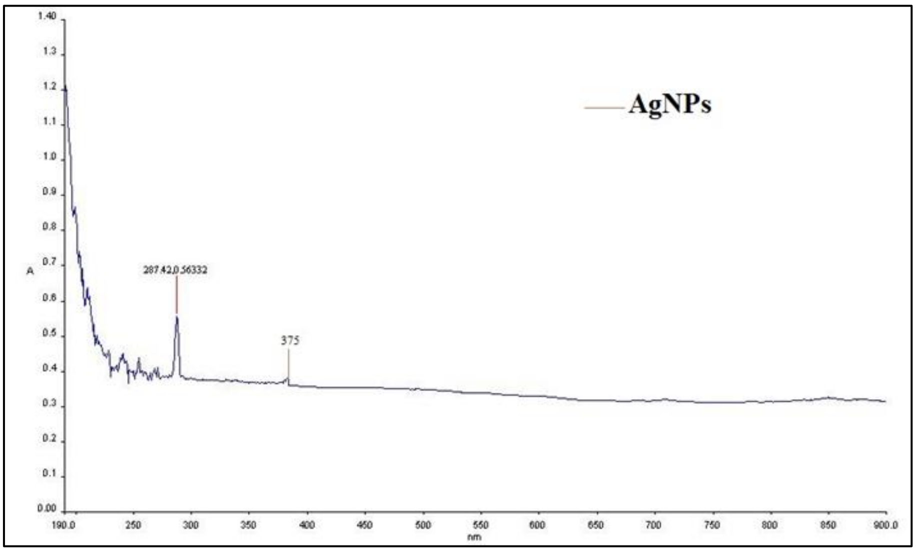

Figure 2 UV/vis Spectrum of the Ag Nanoparticles

From Figure 2, AgNPs' UV/Vis absorbance spectrum showed peak at 287.4 nm and 375 nm. The peak at 287.4 nm occur at lower UV region, showing the systemic electronic transitions. The absorbance peak at 375 nm confirms the complete formation of AgNPs because AgNPs is usually formed at high UV (bathocromic) region, and from that region and above, indicates where materials with possible optical properties are formed [25, 42–44]. This surface plasmon resonance obtained gave more information about the shape, size, and state of aggregation of the NPs and it is close the wavelength max reported in the research carried out by Singh and Navneet [3], and slightly above that observed in the work of Ogwuche and Moses [28]. Since the energy of the absorbed photons can be calculated from the peak and may be used to assess the optical band gap of the NPs, the bandgap (hv/λ) of the AgNPs at 375 nm (lambda max) is 1240/375 = 3.30 eV. This band gap energy value indicates its potential optical property and use in electronics [35, 44].

3.2.2 Fourier Transform Infrared (FTIR) Result of the Ag Nanoparticles

FTIR analysis was used to examine the related functional groups of the biomolecules that serve as capping/stabilizing agents on the surface of AgNPs. An Elmer 3000 MX FTIR spectrometer, with a wave number range of 4500 to 300 (cm^{-1}), was used in this study.

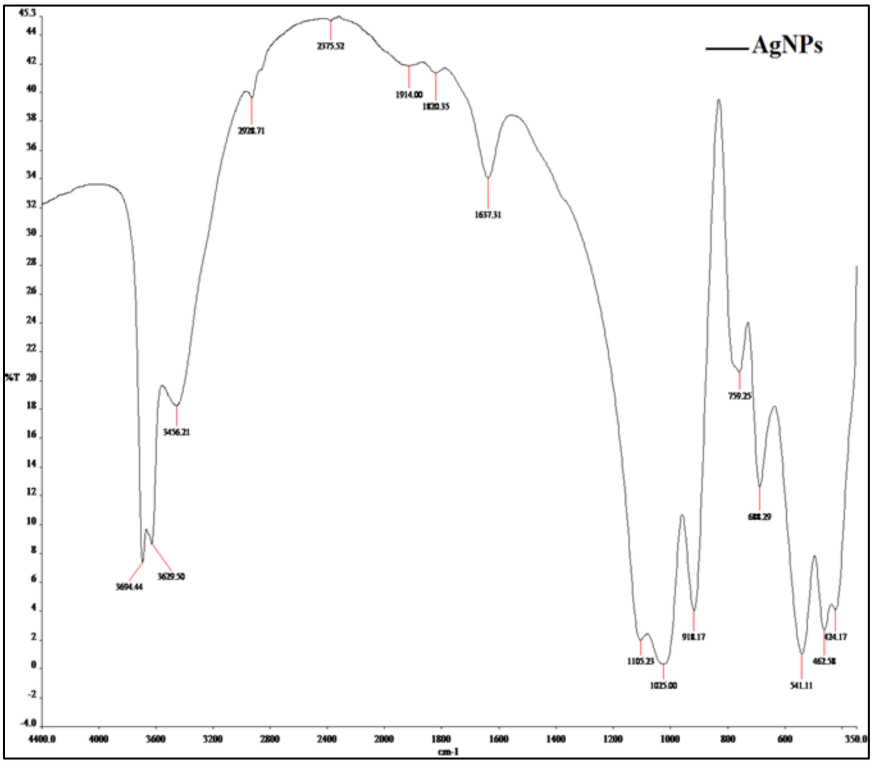

Figure 3 FTIR Spectrum of the Ag Nanoparticles

AgNPs' FTIR revealed bands indicating functional group absorption. The capped silver nanoparticles displayed distinctive peaks at 3694.44, 3629.50, 3456.21, 2928.71, 2800, 2375.52, 1914, 1820.35, 1105.23, 1025, 918.17, 759.29, 688.29, 541.11, 462.58, and 424.17 cm^{-1} for the potential biomolecules that were identified (Figure 4). These bands represent stretched vibrational bands that are in charge of components like alkaloids, terpenoids, glycosides, alkane, and alkyne. The peaks at 3694.44, 3629.50, 3456.21 cm^{-1} represent O–H vibrational stretching of alcohol or phenolic groups [25]. The stretching of primary amine (N–H) is shown at 2928.71 cm^{-1} [45]. The peaks at 2800 and 2375.52 cm^{-1} are attributed to methyl and methylene groups [25], while nitrile group (C≡N) is identified by 1914 cm^{-1} band [44]. The vibration at 1820.35 cm^{-1} corresponds to methoxy (C=O) group, while the ones observed at 1105.23, and 1025 cm^{-1}, indicate the presence of C–O and C–H [25,44]. The sharp peak at 918.17 cm^{-1} is attributed to Ag–O (metal-oxygen) bond, indicating the interaction of the functional group on the NPs' surface [44].

3.2.3 X-ray Diffraction Result of the Ag Nanoparticles

AgNPs' total oxidation status, and crystal structure were examined using a Rigaku D/Max-lllC Powered X-ray diffractometer (pXRD).

As shown in Figure 4, the AgNPs' XRD pattern from *Cissus aralioides* extract revealed its crystalline nature with 2θ values of 24.05°, 27.02°, 28.05°, 40.00°, 46.09°, and 60.07° which are indexed in (100), (111), (101), (200), (220), and (311) face centered cubic planes, respectively. The non-indexed peaks at 9.03°, 22.04°, and 29.09° were associated with the crystallization of bioorganic molecules on the nanoparticles' surface [46–48]. Silver nanoparticle's peak is identified at (111) indexed plane which has a high intensity peak of 27.2° [48]. The diffraction positions showed good level of comparability with the standard values in JCPDS file number 87-0720. Debye-Scherrer formula: $D = K\lambda/\beta\cos\theta$ (where, K = Scherrer constant, λ = the X-ray wavelength, β = the full width at half maximum (FWHM) of the diffraction peak in radians, and θ = the Bragg angle), was used to determine the crystalline size. The calculated size of the AgNPs was 22.52 nm, which fell slightly lower than that obtained by Kanimozhi *et al*. [48], but matches that reported by Ansari *et al*. [49].

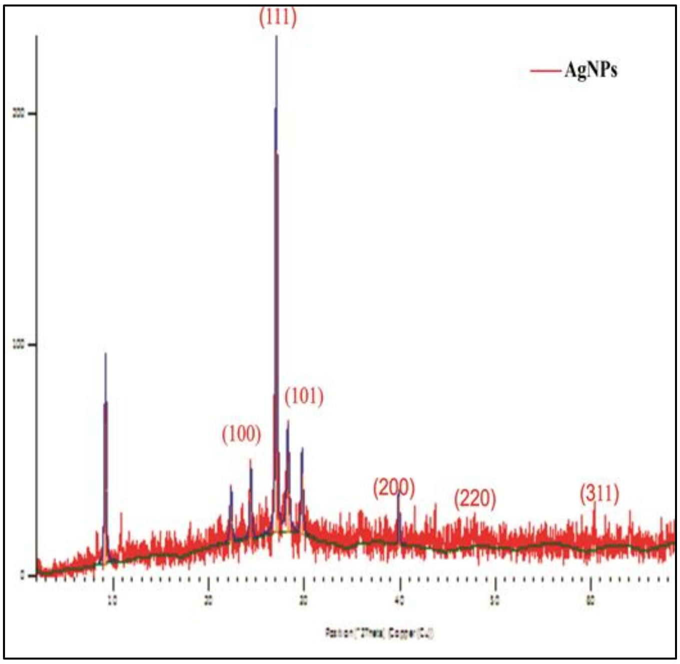

Figure 4 PXRD Spectrum of the Ag Nanoparticles

3.2.4 Scanning Electron Microscope (SEM) Result of the Ag Nanoparticles

Scanning electron microscopy (SEM) was utilized to view the elemental values and the shape of the generated particles at the microscopic level.

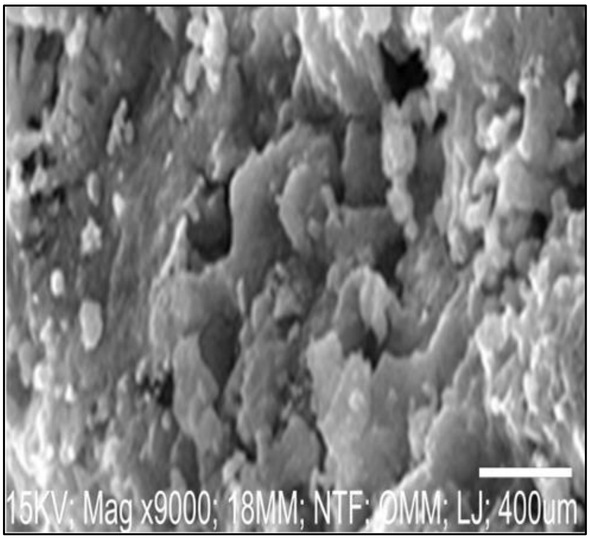

Figure 5 SEM Images of the Ag Nanoparticles

SEM (JOEL JSM-7600F) was used to track the morphological properties of the synthesized silver nanoparticles, and the surface structure and actual morphology of the AgNPs, are displayed (Figure 5). A rough, uneven, and distinctive morphological form was obtained and it shows that the AgNPs has stabilized, presumably as a result of interactions between the NPs' surface and the solution around it. The interactions resulted in the adsorption of the stabilizing agents (functional groups) present in the plant's extract, during the green synthetic process [44].

3.2.5 Energy Dispersive X-ray (EDX) Result of the Ag Nanoparticles

The energy-dispersive X-ray (EDX-8100) machine was used to examine the elemental structure of the generated Ag nanoparticles.

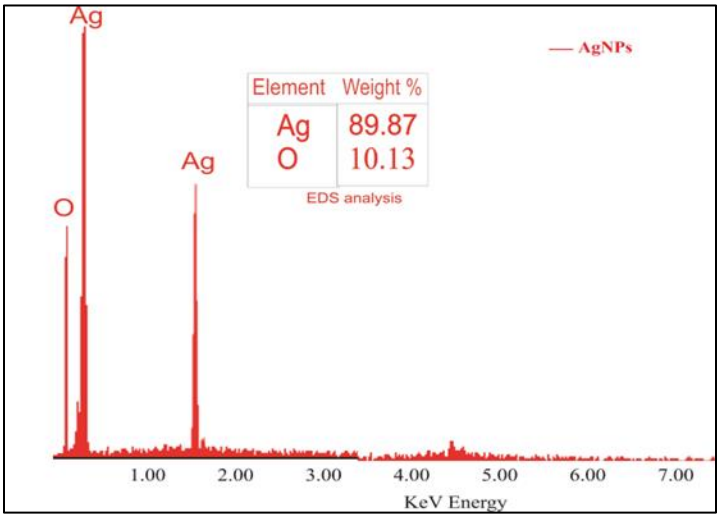

Figure 6 EDX Spectrum of the Ag Nanoparticles

Using the EDX machine (8100), the NPs was exposed to an intense electron beam, and the X-rays it emits were measured. The atomic structure of each of the elements results in unique peaks in the X-ray spectrum since the rays are produced based on the properties of the elements [50–51]. The ratio of the number of X-rays to their energy is the measurement unit. The results from EDX analysis of the biosynthesized AgNPs (Figure 6) showed the presence of various elemental makeup and their percentages, which include silver (89.87%), and oxygen (10.13%) sharp atomic peaks, making up the 100% total. Silver was observed to be the predominant element (Figure 6). The EDX crystal pattern followed that observed in the work of Kasithevar *et al*. [52], and the elemental composition confirms the AgNPs prepared. The EDX values present the chemical makeup, purity, and optical potentials of the nanoparticles [35, 51].

3.2.6 Transmission Electron Microscope (TEM) Results of the Ag Nanoparticles

TEM investigation gives a clear picture of the NPs' form and, more importantly, its particle size. TEM model JEOL2100 apparatus was for this analysis. The mean particle size of the green-synthesized AgNPs was measured using imageJ, and Origin Lab software (version 9.0).

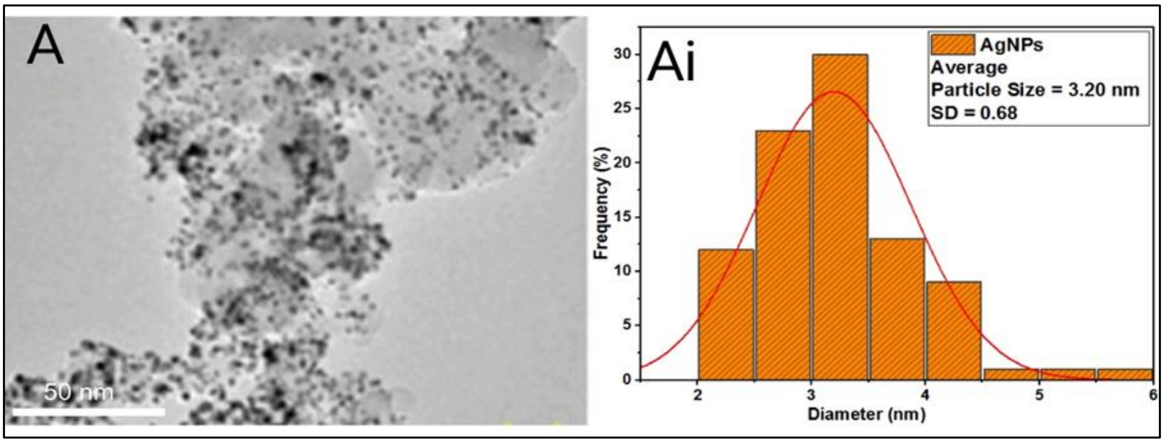

Figure 7 TEM Images of Ag Nanoparticles (A), and Ag Nanoparticles' Average Particle Size from the TEM's image (Ai)

Figure 7A showed the TEM micrograph of a spherical-shaped silver NPs with well-dispersed form and little agglomeration, showing some dark and cloudy areas. This may be attributed to the metal and organic components regions [53–54]. The scale of 50 nm was used to visualize the nanoparticles, and a little overlapping was observed in some areas of the particle's image. The spread in the surface area indicates potentiality of its wide range of applications, especially in adsorption studies [55–56]. The average particle size of the AgNPs as shown in the histogram (Figure 7Ai), as determined by the image resolution analyzer (the ImageJ software), and Origin Lab software, is 3.2 nm. This result is marginally smaller than that reported by Elemike *et al*. [57].

3.3. Antimicrobial Activity Result

The antimicrobial result of the Ag Nanoparticles, is presented below.

Table 2 Antimicrobial activity of the AgNPs

Sample	Microbe	Unit	Concentration			
			400 mg/mL	300 mg/mL	200 mg/mL	100 mg/mL
AgNPs	*E. coli*	mm	10.0±0.04[a]	10.0±0.03[a]	8.0±0.02[b]	8.0±0.01[b]
	S. aureus		20.0±0.01[a]	18.0±0.01[b]	16.0±0.04[c]	16.0±0.01[c]
	C. albicans		22.0±0.04[a]	22.0±0.02[a]	22.0±0.01[a]	18.0±0.04[b]
	Aspergillus sp		22.0±0.01[a]	20.0±0.04[b]	16.0±0.04[c]	16.0±0.01[c]

The values represent Mean±SD; For a Tukey's HSD test, different letters in the same row are significantly different ($p < 0.05$) for each of the parameters evaluated.

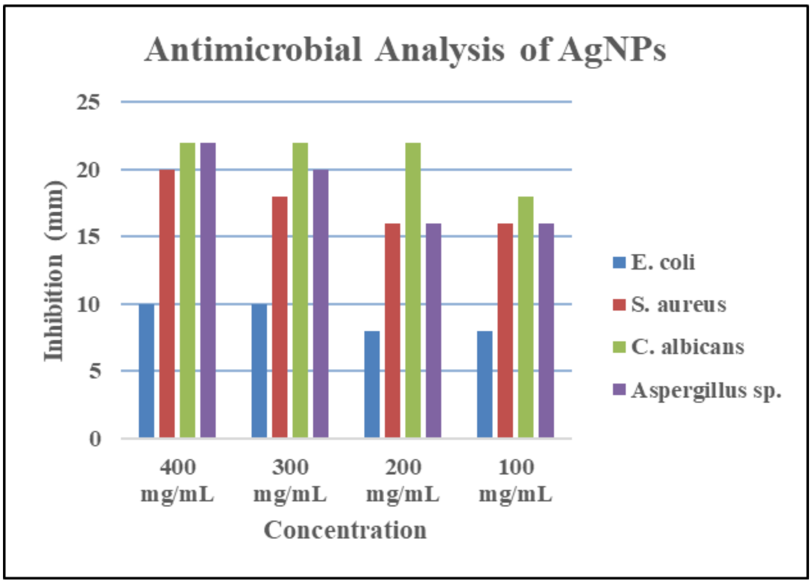

Figure 8 Antimicrobial Result of the AgNPs

Table 2, and Figure 8 showed that the silver nanoparticles from *Cissus aralioides* leaf extract was highly active against all the microbes, with the highest and lowest activity obtained at 22, and 8 mm, respectively. *C. aureus* was more inhibited, displaying sensitivity across the concentrations with 200, 300, and 400 mg/L having 22 mm inhibitory activity, and 18 mm was observed at 100 mg/mL. Following this closely, was the inhibitory effect against *Aspergillus sp.*, which displayed sensitivity across the concentrations at the range of 18-22 mm. While the AgNPs had lowest activity against *E. coli* (at the range of 8 to 10 mm), the inhibitions against *S. aureus* were obtained at 16-20 mm. Many studies have reported activity just over this range [3, 25, 28, 44], and higher than range [58], at the commiserate concentrations.

Table 3 Antibiotics sensitivity result

Control	Microbe	Unit	Concentration			
			50 mg/mL	25 mg/mL	12.5 mg/mL	6.25 mg/mL
Gentamycin	*E. coli*	mm	22.0±0.01[a]	16.0±0.04[b]	13.0±0.04[c]	8.0±0.04[d]
	S. aureus		18.0±0.01[a]	12.0±0.01[b]	10.0±0.01[c]	0.0±0.00[d]
	C. albicans		22.0±0.01[a]	16.0±0.01[b]	13.0±0.01[c]	8.0±0.04[d]
	Aspergillus sp		6.0±0.01[a]	0.0±0.00[b]	0.0±0.00[b]	0.0±0.00[b]

DH2O	*E. coli*	mm	0.0±0.00[a]	0.0±0.00[a]	0.0±0.00[a]	0.0±0.00[a]
	S. aureus		0.0±0.00[a]	0.0±0.00[a]	0.0±0.00[a]	0.0±0.00[a]
	C. albicans		0.0±0.00[a]	0.0±0.00[a]	0.0±0.00[a]	0.0±0.00[a]
	Aspergillus sp		0.0±0.00[a]	0.0±0.00[a]	0.0±0.00[a]	0.0±0.00[a]

The values represent Mean±SD; For a Tukey's HSD test, different letters in the same row are significantly different ($p < 0.05$) for each of the parameter evaluated.

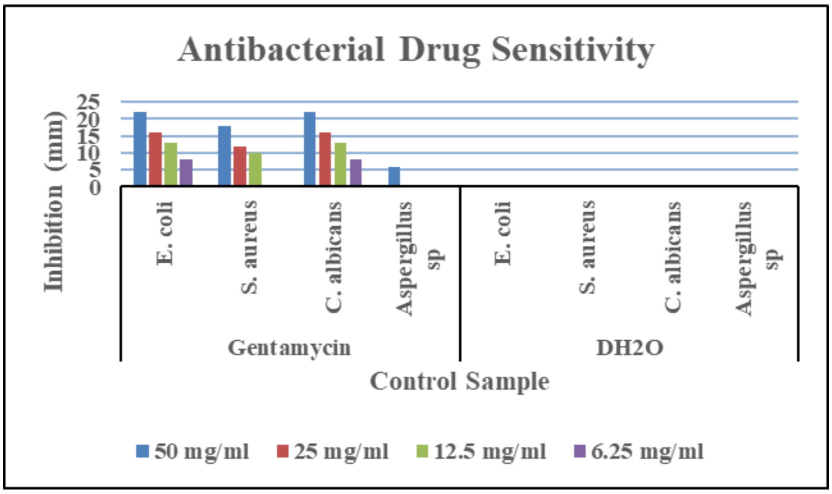

Figure 9 Gentamycin sensitivity result

The AgNPs has close comparison with the positive control, Gentamycin (Table 3, and Figure 9), demonstrating itself as an alternative inhibitory agent against the microbes.

The negative control had no activity against the microbes, confirming there was no contaminants present. The results confirmed that the AgNPs is a promising antimicrobial agent. The increased surface area that enhances improved bioavailability, allowed the nanoparticles to have an enhanced interaction with the enzymes of the microbes, penetrate their cell walls, and induce inhibitory effects to their cellular processes and growth, leading to their cellular damage [30, 44, 59, 60]. AgNPs' cosmetics of this plant has also shown comparability effects [60].

4. Conclusion

The methanol leaf extract of *Cissus aralioides* used in combination with $AgNO_3$ successfully synthesized Ag NPs in this research. It was confirmed that the full synthesis of the NPs was facilitated by the phytochemicals found in the plant extract, which served as stabilizing and capping agents. UV-vis, FTIR, PXRD, SEM, EDX, and TEM instruments used to characterize the NPs confirmed the characteristics results, further affirming its formation. With an estimated bandgap energy of 3.30 eV and a maximum wavelength of 375 nm, the green-synthesized AgNPs was found promising relevance in nanoelectronic applications, as well as semiconductor fabrications. A mean particle size of 3.20 nm was determined from the NPs' TEM image, as well as an average crystalline size of 22.52 nm from PXRD result. Predominant elemental silver found from the EDX result, and the NPs also showed an uneven and rough surface in its SEM data. The plant's abundance of vital phytochemicals with disease-fighting properties is demonstrated by the presence of several functional groups identified by FTIR analysis. Inhibitory activity was observed against *Escherichia coli*, *Staphylococcus aureus*, *Candida albicans*, and *Aspergillus fumigatus* from the antimicrobial activity analysis. Ag nanoparticles demonstrated high activity against all the microbes, with the highest effect (at 22 mm) seen on *C. aureus*. The minimum inhibitory concentration was at 100–200 mg/L. The positive control showed comparable inhibitions but more effective than the sample at increased concentrations. This is a confirmation that the AgNPs was able to cause breakdown in the microbial cell wall, thus demonstrating great inhibitory effects to their biological activities. Overall, the results have demonstrated that the silver nanoparticles can be used to control pathogenic microbes. From the findings, it can be concluded that the synthesized AgNPs has several potential applications, and more especially, can be utilized as antimicrobial agent to control pathogens.

Compliance with ethical standards

Acknowledgments

Tertiary Education Trust Fund (TETFUND) provided funding for the study, and the authors acknowledge them and also thank the management of Nigeria Maritime University, Okerenkoko, and Federal University of Petroleum Resources, Effurun, Delta State, Nigeria, for the platforms provided for the research.

Disclosure of conflict of interest

The authors declare that they have no conflict of interest.

Funding

This study was funded by Tertiary Education Trust Fund (TETFUND) under its Academic Staff Training and Development (AS&D) Batch-D 2023 program.

References

[1] Batista CA, Larson RG, Kotov NA. Nonadditivity of nanoparticle interactions. Sci 2015;350(6257):1242477. https://doi.org/10.1126/science.1242477

[2] Shi J, Kantoff PW, Wooster R, Farokhzad OC. Cancer nanomedicine: Progress, challenges & opportunities. Nat Rev Canc 2017;17(1):20–37. https://doi.org/10.1038/nrc.2016.108

[3] Singh R, Navneet. Green synthesis of silver nanoparticles using methanol extract of Ipomoea carnea Jacq. to combat multidrug resistance bacterial pathogens. Current Res in Green & Sustain Chem 2021;4:10015-10021. https://doi.org/10.1016/j.crgsc.2021.100152

[4] Iravani S, Korbekandi H, Mirmohammadi SV, Zolfaghari B. Synthesis of silver nanoparticles: chemical, physical and biological methods. Res Pharm Sci 2014;9(6):385–406.

[5] Narayanan M, Hussain FAJ, Srinivasan B, Sambantham MT, Al-Keridis LA, AL-mekhlafi FA. Green synthesizes and characterization of copper-oxide nanoparticles by Thespesia populnea against skin-infection causing microbes. J. of King Saud Uni Sci 2022;34(3):101885. https://doi.org/10.1016/j.jksus.2022. 101885

[6] Aghebati-Maleki A, Dolati S, Ahmadi M, Baghbanzhadeh A, Asadi M, Fotouhi A, Yousefi M, Aghebati-Maleki L. Nanoparticles and cancer therapy: Perspectives for application of nanoparticles in the treatment of cancers. J. of Cellul Physiol Wiley Periodicals Inc, 2019;235(3):1962-1972. https://doi.org/10.1002/jcp.29126

[7] Elemike EE, Onunkwo IC, Ughumiakpor O, Alawuru F, Mukoro A, Ishom P, et al. Bio-nanomaterials: Promising anticancer properties and treatment strategies. Nano TransMed 2025;4:100076. https://doi.org/10.1016/j.ntm.2025.100076

[8] Orakwue FC, Maduanusi AB. Phytochemical and antimicrobial screening of methanol extract of Cissus aralioides. Int J of Scientific Innovat 2014;6(1):65-68.

[9] Burkill HM. The useful plants of West Tropical Africa, Families. Royal Botanica. Gardens Kew, 2000;5:301-302.

[10] Aluka P. Plant Database. www.aluka.org/action/showcom-pilationpage?doi=10.5555. 2010. [Accessed November 7, 2023].

[11] Ezeja MI, Omeh YN, Onoja SO, Ukaonu IH. Anti-inflammatory and antioxidant activities of the methanolic leaf extract of Cissus aralioides. Am J of Pharmacolo Sci 2015;3(1):1-6. https:/doi.org/10.12691/ajps-3-1-1

[12] Nwogueze BC, Anachuna KK, Eke CN, Ufearo CS. Toxicity studies and phytochemical screening of aqueous extract of Cissus aralioides plant. J of Adv in Med & Pharma Sci 2018;17(1):1-7.

[13] Assob JC, Kamga HL, Nsagha DS, Njunda AL, Nde PF, Asongalem EA, Njouendou AJ, Sandjon B, Penlap VB. Antimicrobial and toxicological activities of five medicine plant species from Cameroon Traditional Medicine. BMC Complement Altern Med 2011;11:70-75.

[14] Oduje AA, Awode A, Edah A, Sagay I. Characterization and phytochemical screening of n-hexane oil extract from Cissus aralioides seeds Int J of Sci & Eng Res 2015;6(1):112-116.

[15] Al-Mamary M, Al-Habori A, Al-Zubairi AS. The in vitro antioxidant activity of different types of palm dates (Phoenix dactylifera) syrups. Arabian J Chem 2014;6:964-971.

[16] Ren-You GR, Xiang-Rong X, Feng-Lin S, Lei S, Hua-Bin L. Antioxidant activity and total phenolic content of medicinal plants associated with prevention and treatment of cardiovascular and cerebrovascular diseases. J Med Plants Res 2010;4:2438-2444.

[17] Balogun OS, Oladosu IA, Liu Z. Chemical compositions and radical scavenging potentials of essential oils from Tragia benthamii (BAKER) and Cissus aralioides (WELW). Taylor & Francis Group, TBAP 2016;6(1):59–64.

[18] Ezeja MI, Onoja SO, Ukwueze CO, Madubuike GI. Evaluation of the analgesic activity of Cissus aralioides leaves in rat. J of Chemical & Pharma Res 2015b;7(3):2525-2528.

[19] Eze VC, Onoja SO, Chikezie JC. Evaluation of the antimicrobial, antioxidant and phytochemical activities of methanolic and aqueous extract of Cissus aralioides leaves on some selected pathogenic microorganisms. IOSR J of Pharmacy & Biol Sci (IOSR-JPBS) 2015;10(2):32-43.

[20] Anosike CA, Obidoa O, Ezeanyika LUS. The anti-inflammatory activity of garden egg (Solanum aethiopicum) on egg albumin-induced oedema and granuloma tissue formation in rats. Asian Pac J Trop. Med 2012;5(1):62–66.

[21] Anosike CA, Ako AC, Nwodo OFC. Anti-inflammatory and membrane stabilization activities of methanol extract of Cissus aralioides leaves. Res J of Pharm Biol & Chem Sci 2018;18:28.

[22] Nago RDT, Mpetga JDS, Tamokou J-D-D, Fobofou SAT, Bitchagno GTM, Wessjohann LA, Tene M, Ngouela AS. A new ceramide from Cissus aralioides Baker (Vitaceae) and its antimicrobial activity. Chem & Biodiversity 2022;20(1):e202200678. https://doi.org/10.1002/cbdv.202200678

[23] Chaudhary A, Kumar N, Kumar R, Kumar R. Antimicrobial activity of zinc oxide nanoparticles synthesized from Aloe vera peel extract. SN Appl Sci 2019;1(1):136.

[24] Ansari MA, Murali M, Prasad D, Alzohairy MA, Almatroudi A, Alomary MN, Udayashankar AC, Singh SB, Asiri SMM, Ashwini BS, Gowtham HG, Kalegowda N, Amruthesh KN, Lakshmeesha TR, Niranjana SR. Cinnamomum verum bark extract mediated green synthesis of ZnO nanoparticles and their antibacterial potentiality. Biomolecules 2020;10:134–336.

[25] Elemike EE, Ojiefoha OC, Aleruchi C, Hassana LA, Owoseni MC, Mfon R, Enock OD, Adesuji ET. Evaluation of antibacterial activities of silver nanoparticles green-synthesized using pineapple leaf (Ananas comosus). Micron 2013;1-5. http://dx.doi.org/10.1016/j.micron.2013.09.003

[26] Elumalai K, Velmurugan S, Ravi S, Kathiravan V, Ashokkumar S. Green synthesis of zinc oxide nanoparticles using Moringa oleifera leaf extract and evaluation of its antimicrobial activity. Spectrochimica Acta Part A: Molecul & Biomolecul Spectro 2015;143:158–164.

[27] Demissie MG, Sabir FK, Edossa GD, Gonfa BA. Synthesis of zinc oxide nanoparticles using leaf extract of Lippia adoensis (Koseret) and evaluation of its antibacterial activity. J of Chem 2020;7459042. https://doi.org/10.1155/2020/7459042

[28] Ogwuche CE, Moses HO. Characterization, antimicrobial and toxicity studies of silver nanoparticles using Opuntia ficus indica leaves extracts from Effurun, Delta State. Tanzania J of Sci 2021;47(1):34-46. https://dx.doi.org/10.4314/tjs.v47i1.4

[29] Jeong SH, Yeo SY, Yi SC. The effect of filler particle size on the antibacterial properties of compounded polymer/silver fibres. J of Mater Sci 2005;40:5407–5411.

[30] Ahmed KB, Raman T, Veerappan A. Future prospects of antibacterial metal nanoparticles as enzyme inhibitor. Mater Sci Eng C Mater Biol Appl 2016;68:939-47.

[31] Sharma VK, Ria AY, Lin Y. Silver nanoparticles: Green synthesis and their antimicrobial activities. Adv in Colloid & Interface Sci 2009;145:83–96.

[32] Amina R, Aliero B, Gumi M. Phytochemical screening and oil yield of a potential herb, camel grass (Cymbopogon schoenanthus Spreng.). Cent Euro J of Experi Biol 2013;2(3):15b-19.

[33] Jeenu, Joseph L, George M, Bindhu AR. Phytochemical screening and antioxidant activity of various extracts of Clerodendru m., Paniculatum linn. World J of Pharma Res 2018;7(13):555–68.

[34] Onunkwo IC. A handbook of organic chemistry practical: Tests, procedures and results. 1st ed. Warri, Nigeria: XS publishers; 2021.

[35] Akpeji BH, Emegha MC, Onyenue EE, Meshack OQ, Elemike EE. Synthesis and characterization of nanoparticles of ZnO, carbon dot and ZnO-Carbon dot nanocomposite from groundnut shell waste. J Appl Sci Environ Manage 2024;28(6):1771-1780.

[36] Banala RR, Nagati VB, Karnati PR. Green synthesis and characterization of Carica papaya leaf extract coated silver nanoparticles through X-ray diffraction, electron microscopy and evaluation of bactericidal properties. Saudi J of Biol Sci 2015;22:637–644.

[37] Elemike EE, Onwudiwe DC, Mbonu JI. Facile synthesis of cellulose–ZnO-hybrid nanocomposite using Hibiscus rosa-sinensis leaf extract and their antibacterial activities. Appl Nanosci 2021;11(4):1349–1358. https://doi.org/10.1007/s13204-021-01774-y

[38] Zainab, Khan MS, Ahmad M, Khan MA, SobiIn. In vitro antimicrobial activity of Rumex Dentatus L. (Polygonaceae) plant extracts. Phytopharmacol Res J 2022;1(3):32-42.

[39] Borokini TI, Omotayo FO. Comparative phytochemical analysis of selected medicinal plants in Nigeria. Intl J of Adv Chem Res 2015;1(1):011-018.

[40] Muhamad M., Ai Sze W., Zulkifli, N. S., Ab-Rahim S. Qualitative analysis on the phytochemical compounds and total phenolic content of Cissus hastata (Semperai) leaf extract. Int J Plant Biol 2023;14:53–62. https://doi.org/10.3390/ijpb14010005

[41] Zhao X, Hu X, Xie Q, Qi S, Xiang Z, Sun X, Xie Z, Dang R, Zhou L, Liu W, Cheng X, Wang C. Ameliorative effect of scopolamine-induced cognitive dysfunction by Fufangmuniziqi formula: The roles of alkaloids, saponins, and flavonoids. J Ethnopharmacol 2024; 318(Pt A):116792. https://doi.org/10.1016/j.jep.2023.116792

[42] Prakash P, Gnanaprakasam P, Emmanuel R, Arokiyaraj S, Saravanan M. Green synthesis of silver nanoparticles from leaf extract of Mimusops elengi, Linn. for enhanced antibacterial activity against multi drug resistant clinical isolates. Colloids Surf B Bioint 2013;108:255-9.

[43] Wang C, Kim YJ, Singh P, Mathiyalagan R, Jin Y, Yang DC. Green synthesis of silver nanoparticles by Bacillus methylotrophicus, and their antimicrobial activity. Artif Cells Nanomed Biotechnol 2016;44:1127-32.

[44] Bawazeer S. Green synthesis of silver nanoparticles from Euphorbia milii plant extract for enhanced antibacterial and enzyme inhibition effects. Int J of Health Sci 2024;18(2):18-25.

[45] Din MI, Jabbar S, Najeeb J, Khalid R, Ghaffar T, Arshad M, Khan SA, Ali S. Green synthesis of zinc ferrite nanoparticles for photocatalysis of methylene blue. Int J of Phytoremed 2020;22(13):1440-1447. https//doi.org/ 10.1080/15226514.2020.1781783

[46] Mallikarjuna K, John Sushma N, Narasimha G, Manoj L, Deva Prasad Raju B. Phytochemical fabrication and characterization of silver nanoparticles by using Pepper leaf broth. Arab J Chem 2014;7(6):1099–1103.

[47] Gomathi M, Rajkumar PV, Prakasam A, Ravichandran K. Green synthesis of silver nanoparticles using Datura stramonium leaf extract and assessment of their antibacterial activity. Resour-Effic Technol 2017;3(3):280–284.

[48] Kanimozhi S, Durga R, Sabithasree M, Kumar AV, Sofiavizhimalar A, Kadam AA, Rajagopal R, Sathya R, Azelee NIW. Biogenic synthesis of silver nanoparticle using Cissus quadrangularis extract and its invitro study. J of King Saud Uni – Sci 2022;34:101930.

[49] Ansari M, Ahmed S, Abbasi A, Khan MT, Subhan M, Bukhari NA, Hatamleh AA, Abdelsalam NR. Plant mediated fabrication of silver nanoparticles, process optimization, and impact on tomato plant. Sci Reports 2023;13:18048. www.nature.com/scientificreports/ https://doi.org/10.1038/s41598-023-45038-x

[50] Geetha MS, Nagabhushana H, Shivananjaiah HN. Green mediated synthesis and characterization of ZnO nanoparticles using Euphorbia Jatropa latex as reducing agent. J Sci Adv Mater Devices 2016;1(3):301–310.

[51] Al-darwesh MY, Ibrahim SS, Mohammed MA. A review on plant extract mediated green synthesis of zinc oxide nanoparticles and their biomedical applications. Results in Chem 2024;7:101368. https://doi.org/10.1016/j.rechem.2024.101368

[52] Kasithevar M, Saravanan M, Prakash P, Kumar H, Ovais M, Barabadi H, Shinwar ZK. Green synthesis of silver nanoparticles using Alysicarpus monilifer leaf extract and its antibacterial activity against MRSA and CoNS isolates in HIV patients. J of Interdiscipl Nanomed 2017;2(2):131-141. https://doi.org/10.1002/jin2.26

[53] Ogwuche CE, Elemike EE, Oju D, Singh ODCM, Akpeji BH. Synthesis, characterization, anticancer and antimicrobial potentials of Chrysothemis pulchella leaf extract mediated gold nanoparticles. J Inorg Organomet Polym Mater 2023. https://doi.org/10.1007/s10904-023-02817-3

[54] Akpeji BH, Bawa HA, Gbajabiamila AT, Elemike EE, Ogunsipe A, Amitaye AN, Hossain I, Aziza AE. Nanocomposites of tin hydroxide phthalocyanine Sn(OH)2Pc and titanium dioxide nanoparticles for improved antimicrobial activities. J of Inorganic & Organometall Polymers & Mater 2024c;35:1292-1308. https://doi.org/10.1007/s10904-024-03291-1

[55] Tratnyek PG, Johnson RL. Nanotechnologies for environmental cleanup. Nano today, 2006;1:44. http://dx.doi.org/10.1016/S1748-0132(06)70048-2

[56] Akpeji BH, Laric B, Igbukud UA, Tesie GO, Elemike EE, Akusu PO. Synthesis and characterization of MnO_2 nanoparticles mediated by Raphia hookeri seed. J Nig Soc Phys Sci 2024b;6:2203.

[57] Elemike EE, Fayemi OE, Ekennia AC, Onwudiwe DC, Ebenso EE. Silver nanoparticles mediated by Costus afer leaf extract: synthesis, antibacterial, antioxidant and electrochemical properties. Molecules 2017;22:701. https://doi.org/10.3390/molecules22050701

[58] Rao NH, Lakshmidevi N, Pammi SVN, Kollu P, Ganapaty S, Lakshmi P. Green synthesis of silver nanoparticles using methanolic root extracts of Diospyros paniculata and their antimicrobial activities. Mater Sci Eng 2016;62C:553–557.

[59] Salleh A, Naomi R, Utami ND, Mohammad AW, Mahmoudi E, Mustafa N, et al. The potential of silver nanoparticles for antiviral and antibacterial applications: A mechanism of action. Nanomaterials (Basel) 2020;10:1566.

[60] Onunkwo IC, Edema MO, Ogwuche CE. Cissus araliodes: cosmetology application of the methanol extract, its silver and zinc oxide nanoparticles and characterization. Chem Papers 2026. https://doi.org/10.1007/s11696-026-04658-z